diversity

Article

Morphological Variability of *Alveolophora antiqua* from a Freshwater Early Miocene Paleolake in the Barguzin Valley (Baikal Rift Zone)

Marina Usoltseva [1,*], Lyubov' Titova [1], Abdulmonem Hassan [2,3], Sergei Rasskazov [2,4] and Alexey Morozov [1]

1 Limnological Institute of the Siberian Branch of the Russian Academy of Sciences, 3 Ulan-Batorskaya, Irkutsk 664033, Russia
2 Institute of the Earth's Crust of the Siberian Branch of the Russian Academy of Sciences, 128 Lermontova, Irkutsk 664033, Russia
3 Geology Department, Faculty of Science, Al-Baath University, Homs PB 77, Syria
4 Geological Faculty, Irkutsk State University, 3 Lenin, Irkutsk 664003, Russia
* Correspondence: usmarina@inbox.ru

Abstract: Using scanning electron microscopy, the morphology of *Alveolophora antiqua* (Moisseeva) Moisseeva from the freshwater Early Miocene paleolake in the Barguzin Valley was studied. We extended the species diagnosis relative to features such as spines, structure of areolae, costae, alveolae, rimoportulae and the external opening of rimoportulae and show a wide morphological variability with regard to valve shape (round, oval, ovoid and triangular). The percentage of these shapes varied with the core depth. Oval valves dominated in lower layers, while triangular ones occur in upper layers. We propose that the shape variability of valves might be due a sharp short-term cooling event or polyploidization. The finding of *A. antiqua* in the Early Miocene deposits of the Barguzin Valley expands both the georaphic and stratigraphic ranges of this species.

Keywords: *Alveolophora antiqua*; fossil diatoms; Miocene; oval; triangular valves; Barguzin Valley

Citation: Usoltseva, M.; Titova, L.; Hassan, A.; Rasskazov, S.; Morozov, A. Morphological Variability of *Alveolophora antiqua* from a Freshwater Early Miocene Paleolake in the Barguzin Valley (Baikal Rift Zone). *Diversity* **2022**, *14*, 1075. https://doi.org/10.3390/d14121075

Academic Editor: Davide Bassi

Received: 3 November 2022
Accepted: 2 December 2022
Published: 5 December 2022

1. Introduction

The Barguzin Valley is the largest intermountain depression located between the Barguzin and Ikat ridges to the northeast of the Svyatoy Nos Peninsula and Barguzin Bay of Lake Baikal (Figure 1). It is one of the axial structures of the Baikal Rift Zone.

We started the study of diatoms from the Miocene–Pliocene deposits of the Barguzin Valley in 2012. Since then, diatoms from cores 532, 531 and 545 have been studied [1–3].

The freshwater diatom genera *Aulacoseira* Thwaites, *Alveolophora* Moisseeva et Nevretdinova, *Pseudoaulacoseira* Lupikina et Khursevich and *Actinocyclus* Ehrenberg dominated in these cores. The latter three genera are extinct. Among *Alveolophora* the species *A. tscheremissinovae* Khursevich, *A. baicalensis* Khursevich et Fedenya, *A. jouseana* (Moisseeva) Moisseeva and *A. antiqua* (Moisseeva) Moisseeva have been identified in the Barguzin Valley.

The most ancient *Alveolophora* species are *A. jouseana* and *A. antiqua*. *Alveolophora antiqua* was described from the Lower–Middle Miocene deposits of the Vitim Plateau (Transbaikalia) [4,5]. Later, *A. antiqua* was also mentioned in Upper Miocene deposits from Lake Baikal [6]. In both cases, this species was recorded but not studied with scanning electron microscopy (SEM).

Although, while describing this species, A.I. Moisseeva noticed that "by the character of the structure of the valve outer face and the curve, the species is very similar to *A. jouseana* with noticeable difference mainly by valves shape. However, complete absence at present of data on the structure of *A. antiqua* allows only to suppose the close relation of these species".

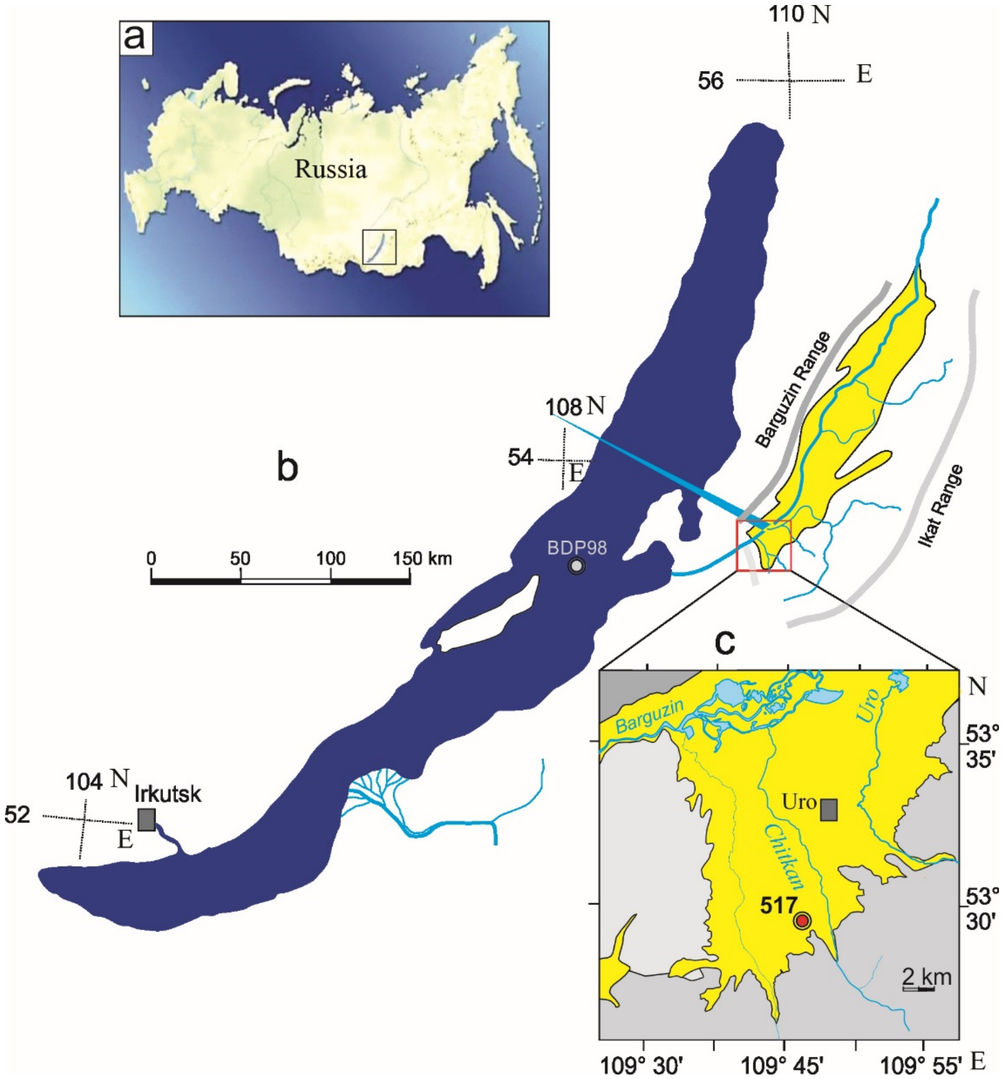

Figure 1. The location of the Lake Baikal (**a**), Barguzin Valley in the Baikal rift zone (**b**) and the location of core 517 (Uro area) (**c**).

While studying the diatoms from the Barguzin Valley, we found that *A. antiqua* dominated throughout the entire core 517.

The purpose of the current work was to study the morphological variability of *A. antiqua* in the core using scanning electron microscopy and to compare this with other similar species in the genus.

2. Materials and Methods

Samples were taken from 44.5, 46, 48, 53, 54, 55, 59 and 61 m of the core 517 (53°30′00″ N; 109°46′53.38″ E) drilled on the southeast of Barguzin Valley by Baikal Branch of Sosnovgeology "Urangeologorazvedka". They were represented by light gray homogeneous siltstone and contained an abundant amount of diatoms (Figure 2). The Early Miocene age of these sediments was stated before by the results of the palynological analysis [7].

The preparation of samples for light microscopy and quantitative accounting was carried out according to the method described in [8]. Cleaned valves were dried on cover slips and mounted in Naphrax (Naphrax Ltd., Bedford, UK, refractive index = 1.74) UK, refractive index = 1.74) and counted using an Axiovert 200 ZEISS LM (Carl Zeiss, Jena, Germany) light microscopy equipped with a Pixera Penguin 600CL camera. For scanning electron microscopy, diatom frustules were broken by crushing a drop of the material between two cover glasses. The material was then placed on a stub and coated with gold using a SDC 004 (BALZERS) ion sputter for 150 s at 10–15 mA. The sample was analyzed using a SEM Quanta 200 (FEI Company, Hillsboro, OR, USA) at 21.5 kV and 10 mm working distance.

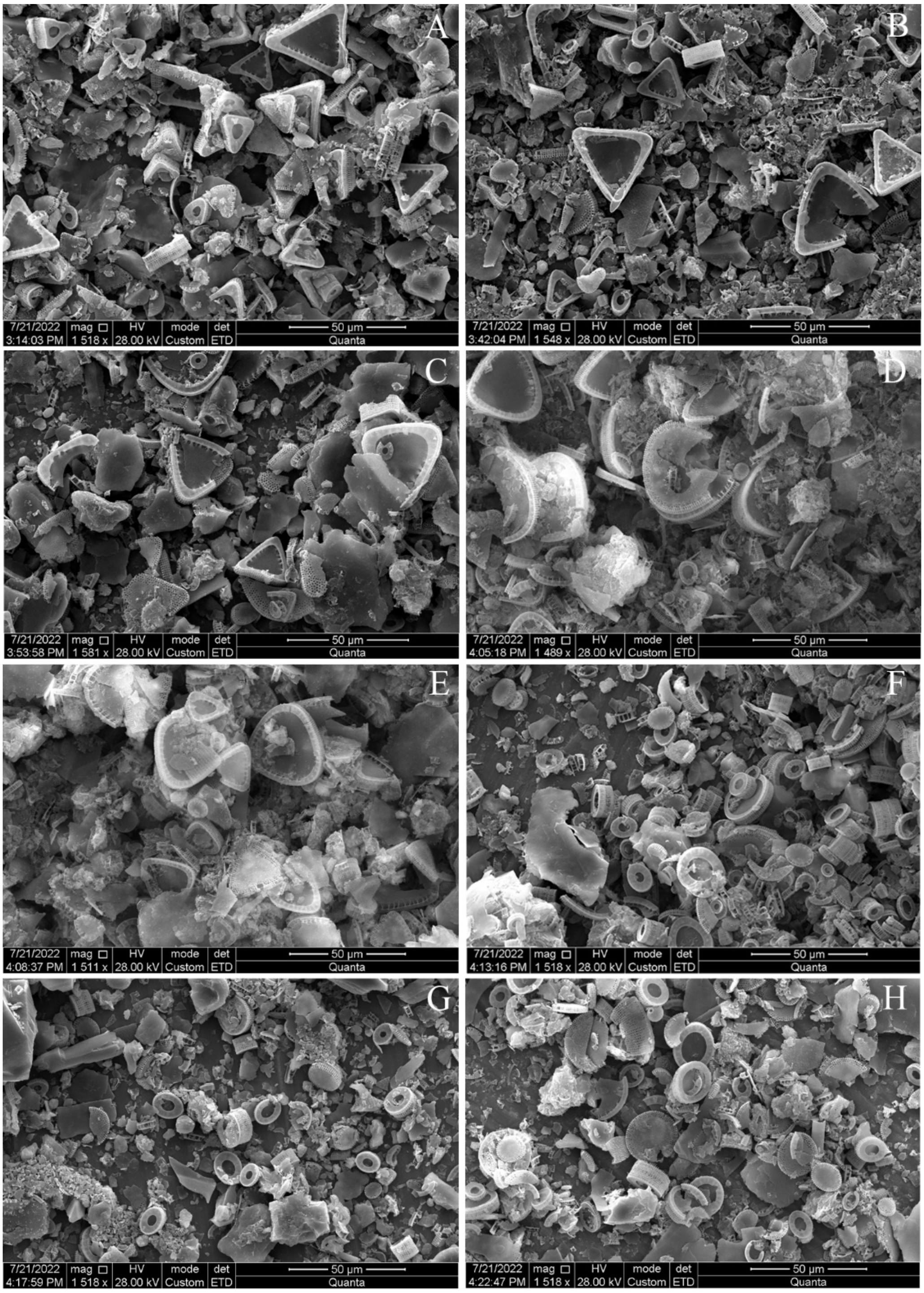

Figure 2. Samples of core 517 used for valve morphology analysis in SEM. (**A**)—44.5 m; (**B**)—46 m; (**C**)—48 m; (**D**)—53 m; (**E**)—54 m; (**F**)—55 m; (**G**)—59 m; (**H**)—61 m.

The features shown in Figure 3 were used for morphometric analysis. A total of 406 diatom valves were measured.

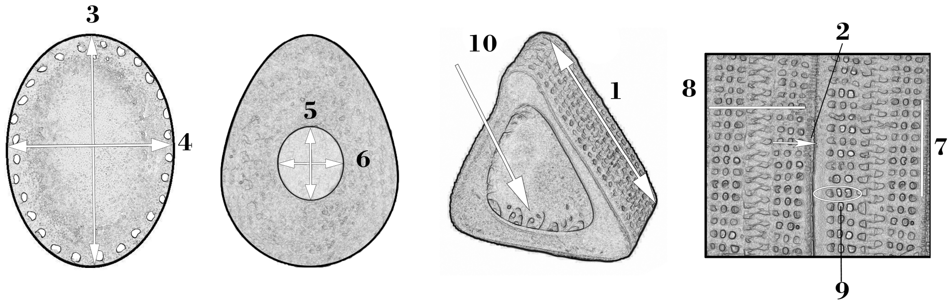

Figure 3. Morphometric features of *Alveolophora antiqua*: 1—length of side face; 2—valve height; 3—valve diameter by apical axis (a.a); 4—valve diameter by transapical axis (t.a); 5—diameter of the ringleist aperture by apical axis; 6—diameter of the ringleist aperture by transapical axis; 7—number of areolae rows in 10 µm; 8—areolae number in 10 µm of a row; 9—areolae number in a row; 10—costae number in 10 µm.

The data were plotted using Microsoft Excel, Corel Draw 16 and Grapher 14. A box-and-whiskers plot was built in Python3 using Matplotlib [9].

3. Results

In core 517, the diatoms occurred in a depth range of 61 to 44.5 m (Figure 4). The absolute dominant species along the whole core was the planktonic diatom *A. antiqua*. The relative abundance of this species ranged between 89–99% of the total number of diatoms. The maximum abundance (910.7 million valves/g) was found at a depth of 48 m, while the minimum abundance—33.9 million valves/g—was found at a depth of 46 m.

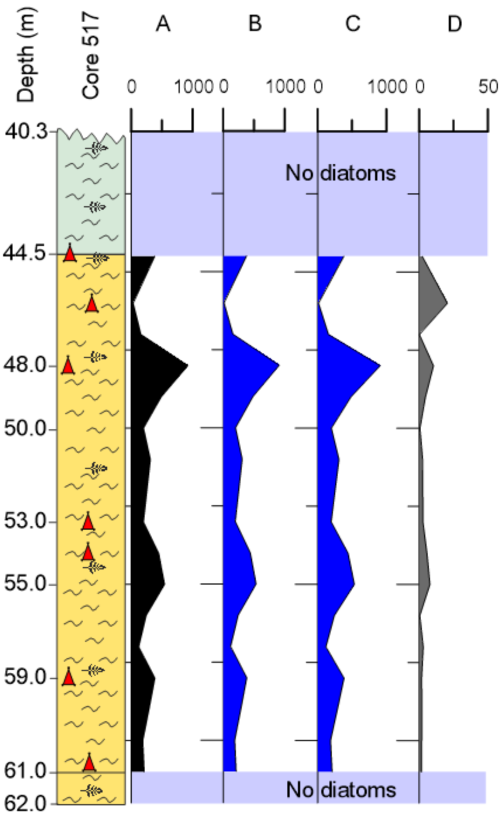

Figure 4. Quantitative distribution of *Alveolophora antiqua* in core 517: A—the number of diatoms (million valves/gram); B—the number of planktonic diatoms; C—the number of *A. antiqua*; D—the number of benthic diatoms. Triangles in the lithological column show sampling depths for palynological analysis.

The study results show a wide morphological variability in *A. antiqua* with regard to valve shape. For this species, round, oval, ovoid and triangular valves were revealed. The percentage of valves of different shapes related to core depth is shown in Figure 5.

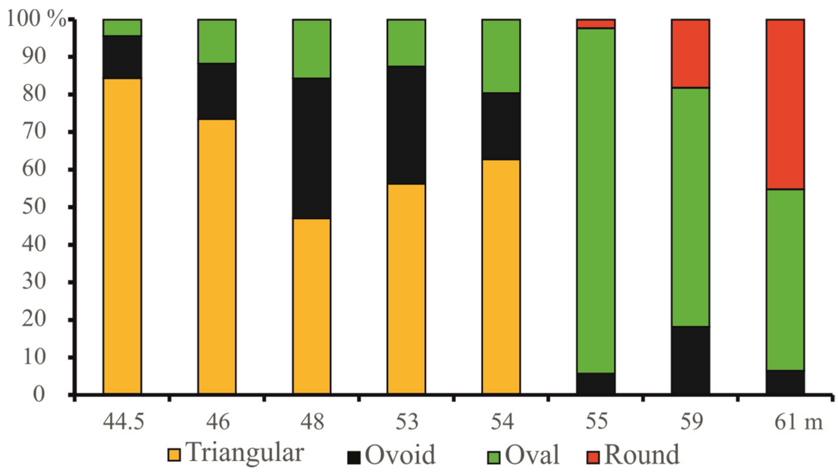

Figure 5. Percentage of different valves shapes of *Alveolophora antiqua* in core 517.

The figure suggests that the upper part of the core (44.5–54 m) was dominated by triangular valves (47–84%). The ovoid valve fraction was 11–37%, while the oval valves were present in the range of 4 to 19%. Oval valves dominated at a depth of 55–61 m; their fraction was 48–92%. The amount of ovoid ones was small (6–18%). The maximum amount of round valves (45%) was found at the depth of 61 m. Upward in the core (59 and 55 m), their amount considerably decreased (18 and 2%, respectively), and below a depth of 54 m, they disappeared completely.

Both the shape and size of valves varied upward in the core (Figures 2 and 6).

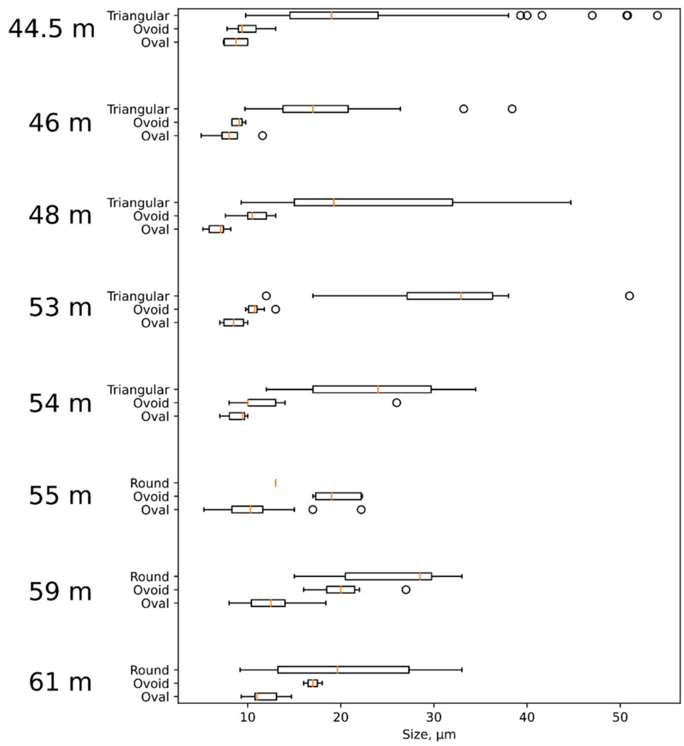

Figure 6. The distribution of *Alveolophora antiqua* valves of different shapes by size in core 517. For round valves, we measured the diameter; for oval ones—larger diameter; for triangular ones—a valve.

Valve size varied greatly in triangular-shaped *A. antiqua* in the upper part (48–44.5 m) of the core. In the middle part of the core, this valve size was less than in the upper one but slightly more than in the lower part. The sizes of ovoid and oval valves decreased upward in the core.

Thus, by valve size and shape, all samples can be divided into three groups. The first one is the depth range of 61 to 55 m, and it includes round, oval and ovoid valves. The second one is transitional, in the range of 54 to 53 m, and it includes oval, ovoid and triangular valves of medium size. The third group is the range of 48 to 44.5 m, and it includes oval, ovoid and triangular valves with a wide range of valve size.

Using SEM, we studied the valve morphology and ultrastructure from these three ranges (61–55, 54–53 and 48–44.5 M).

In the depth range of 61 to 55 m, we found round (Figure 7A,B,D,E,K), ovoid (Figure 7C,F–J,L,N–P) and oval (Figure 7H,I,M,Q,R) valves of *A. antiqua*.

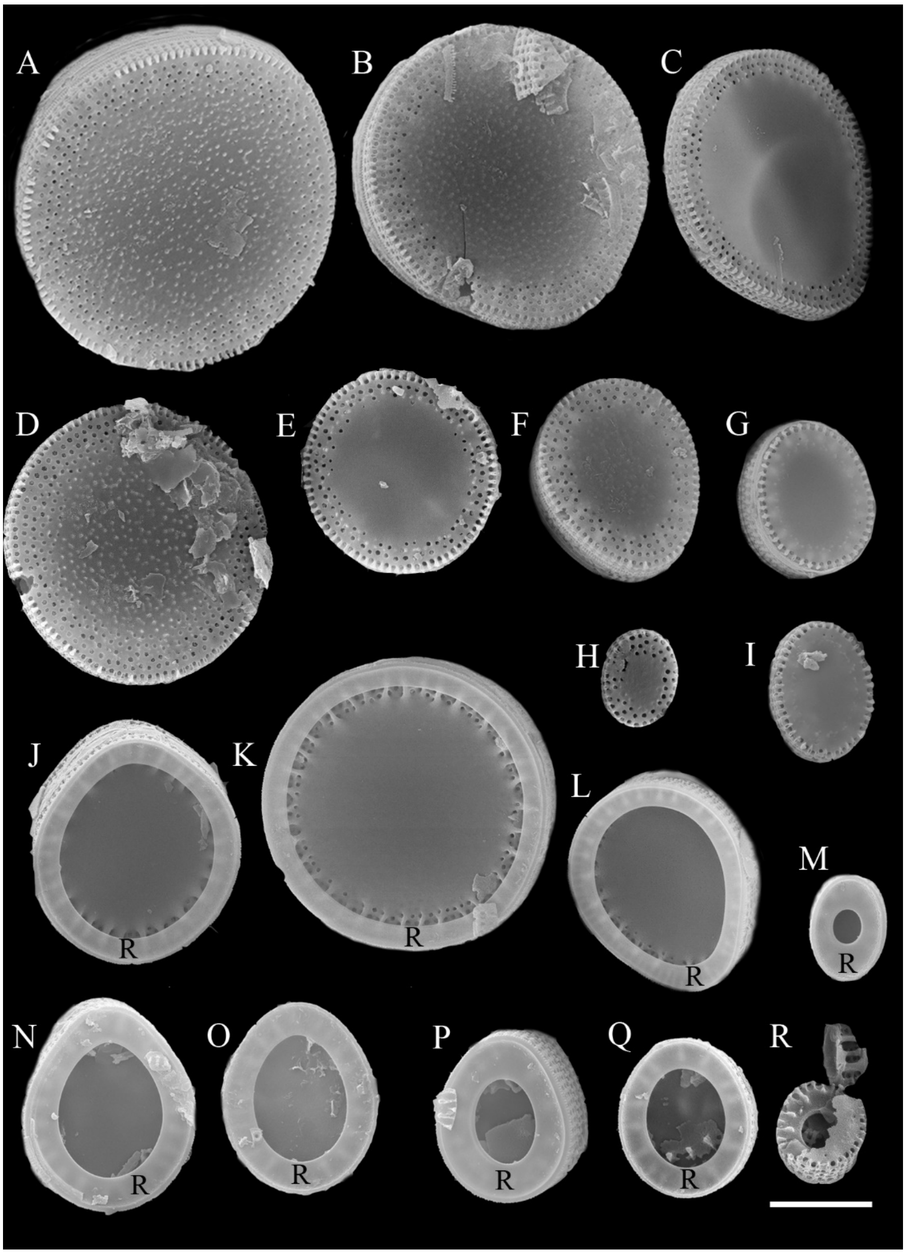

Figure 7. *Alveolophora antiqua* in the depth interval of 61–55 m from core 517 of the Barguzin Valley: (**A**–**I**)—external views, valve face; (**J**–**R**)—internal views showing a ringleist (R), variability of valves and aperture of ringleist in their shape. SEM. Scale bar: 10 µm.

The outer face of the valve is smooth in the center (Figure 7C,E,G–I), or it is covered with small granules (Figure 7A,B,D,F). The areolae along the edge of valve face are situated in 1–4 rows (Figure 7A–F,H) or are not available (Figure 7G,I). Ringleist varies from narrow (Figure 7J–L,R) to medium-size (Figure 7N,O,Q,P) to wide (Figure 7M,P,R). Round areolae are located on the mantle in straight rows (Figure 8A–F). Areolae have 5–6 volae running to the center, from the inside—a bell–like plate with radial perforations attaches to them (Figure 8C,E,G–I). Linking spines are spatulated (Figure 8A,B,D,F). No separating spines were found at the valves in this horizon. Well-developed alveolae interzones are seen from the inner part of the valve (Figure 8I,J). Rimoportulae are sessile and occur at the base of the alveola interzone (Figure 8I,J). Their external opening are associated with the first areola of the row (Figure 8C,E,G).

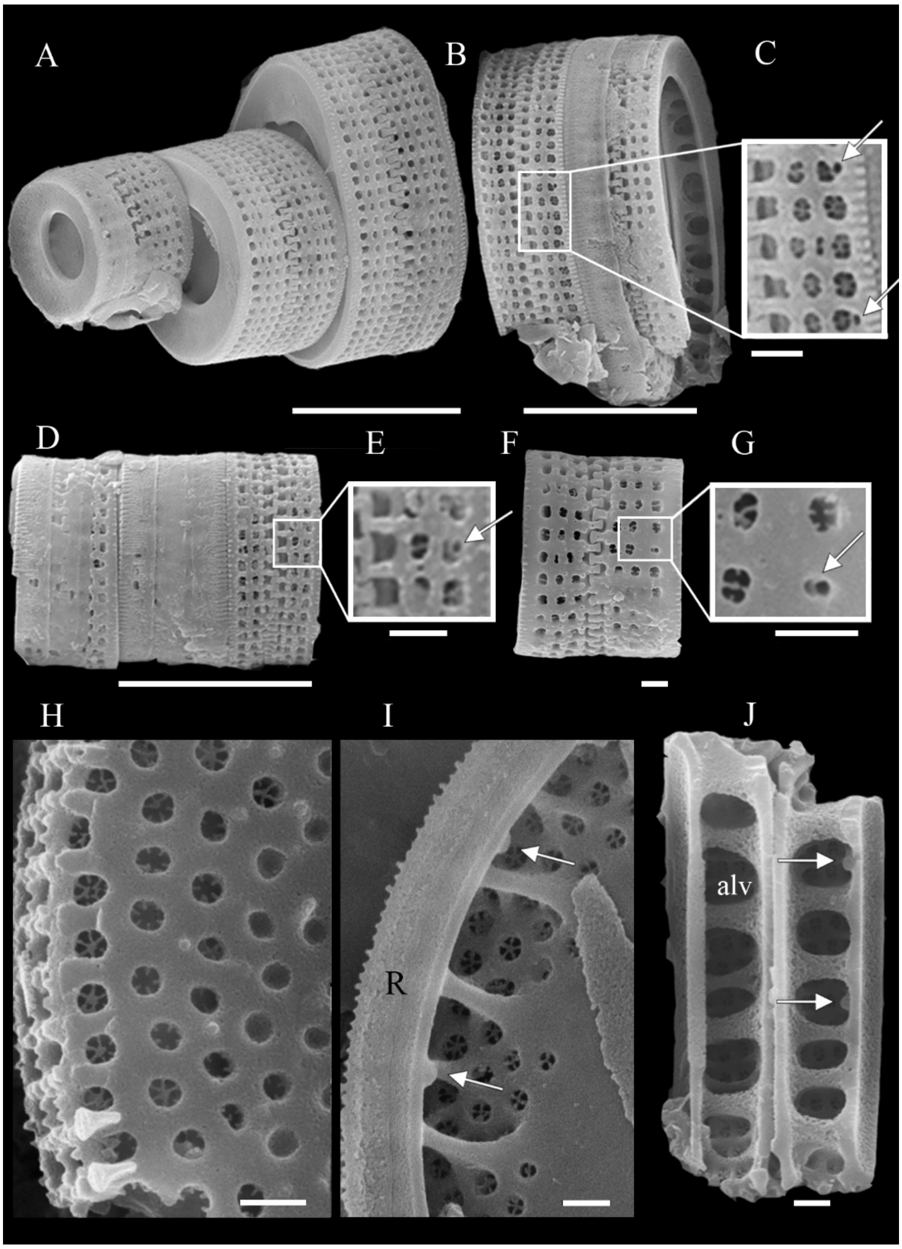

Figure 8. *Alveolophora antiqua* in the depth range of 61 to 55 m from core 517 of the Barguzin Valley: (**A**,**B**,**D**,**F**)—external views, showing variability of valves; (**C**,**E**,**G**)—fragments of valves, showing areolae and external opening of rimoportulae; **H**—areolae on the valve face; (**I**,**J**)—internal views showing a ringleist (R), areolae, rimoportulae (arrows) and alveolae. SEM. Scale bar: 10 µm (**A**,**B**,**D**) and 1 µm (**C**,**E**–**J**).

In the depth range of 54 to 53 m, we found triangular-shaped valves with widely rounded corners, round–triangular (Figure 9A–D), triangular (Figure 9B in the upper part, E–H), ovoid (Figure 9I–K) and oval (Figure 9L,M) valves of *A. antiqua*. The outer face of the valve is covered in the center with small granules (Figure 9C). The areolae along the edge of the valve face are situated in 1–4 rows (Figure 9C) or are not present (Figure 9I).

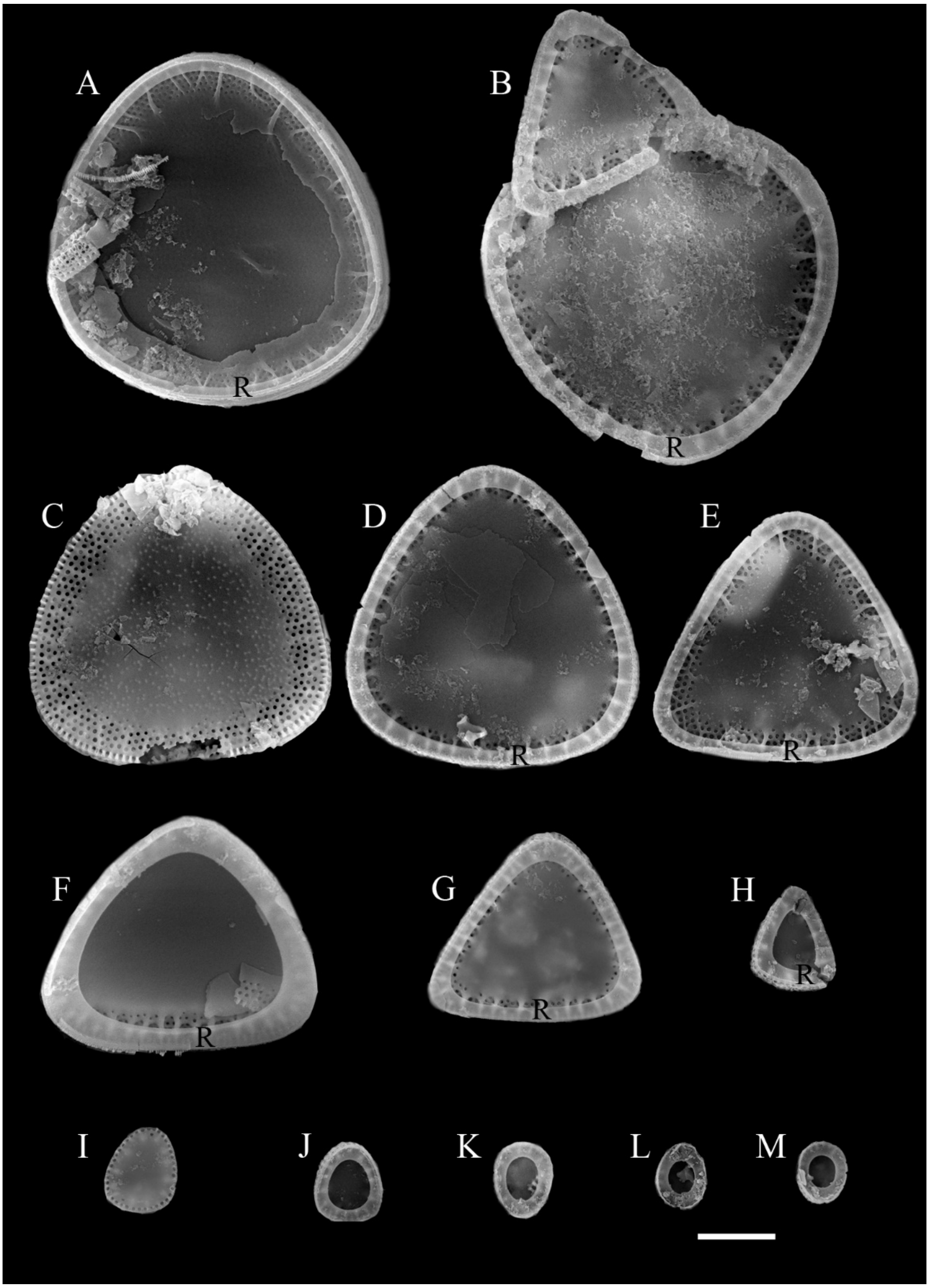

Figure 9. *Alveolophora antiqua* in the depth range of 54 to 53 m from core 517 of the Barguzin Valley: (**A**,**B**,**D**–**M**)—internal views showing a ringleist (R), variability of valves and aperture of ringleist in their shape; (**C**)—external view of the valve face. SEM. Scale bar: 10 µm.

The ringleist varies from narrow (Figure 10A,B,D,E,G) to medium width (Figure 10F,I) and wide (Figure 10H,J–M). Round areolae are located on the mantle in straight rows (Figure 10A–F). Areolae have 5–6 volae running to the center from the inside—a bell–like plate with radial perforations attached to them (Figure 10G,H). Linking spines are spathulate (Figure 10D,E). Separating spines are elongated and petaloid (Figure 10E,F). Well-developed alveola interzones are seen inside the valve (Figure 10H–J). Rimoportulae are sessile and occur at the base of the alveola interzone (Figure 10I,J). Their external opening are associated with the first alveola in the row (Figure 10E).

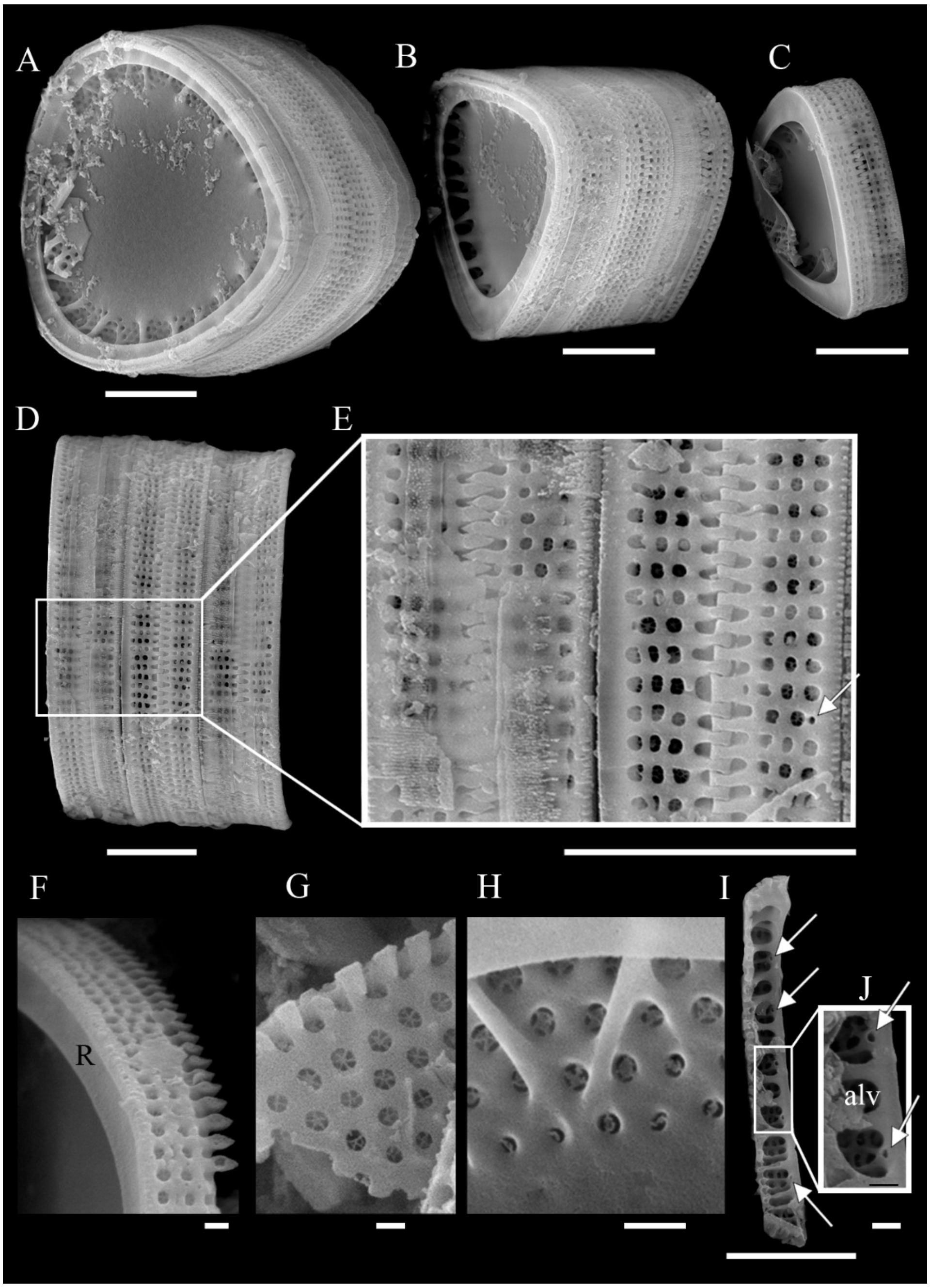

Figure 10. *Alveolophora antiqua* in the depth interval of 54–53 m from core 517 of the Barguzin Valley: (**A**–**D**)—external views, showing variability of valves; (**E**)—fragment of valve D, showing areolae, separating and linking spines, external opening of rimoportulae; (**F**)—separating spines; (**G**)–areolae on the valve face; (**H**)—internal views showing, areolae and costae; (**I**,**J**)—internal view, showing alveolae and rimoportulae (arrows). SEM. Scale bar: 10 µm (**A**–**E**,**I**) and 1 µm (**F**–**H**,**J**).

In the depth range of 48 to 44.5 m, we found triangular (Figure 11A–C,G–K), ovoid (Figure 11L–N) and oval (Figure 11D,O) valves *A. antiqua*. The outer face of the valve is smooth in the center (Figure 11A). The areolae along the edge of face valve are in 1–4 rows (Figure 11A) or are not available (Figure 11D).

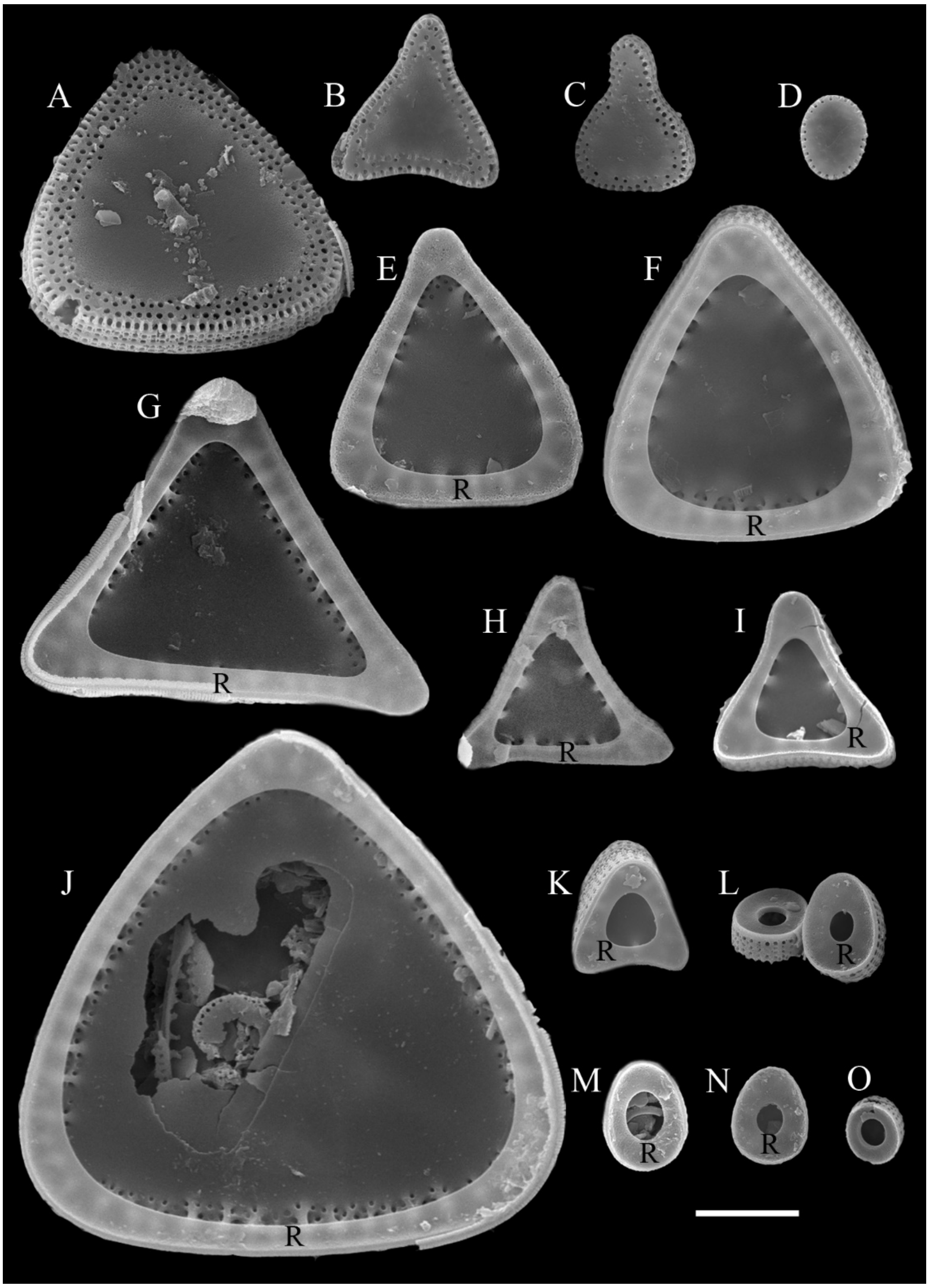

Figure 11. *Alveolophora antiqua* in the depth interval of 48–44.5 m from core 517 of the Barguzin Valley: (**A**–**D**)—external views, valve face; (**E**–**O**)—internal views showing a ringleist (R), variability of valves and aperture of ringleist in their shape. SEM. Scale bar: 10 µm.

The ringleist varies from narrow (Figure 11J) to medium (Figure 11E–I) to wide (Figure 11K–O). Round areolae are located on the mantle in straight rows (Figure 12A–F). Linking spines are spathulate (Figure 12A–E). Separating spines were not found on the valves in this horizon. Well-developed alveola interzones are seen inside the valve

(Figure 12F–J). Rimoportulae are sessile and located at the base of alveola interzone (Figure 12G–J).

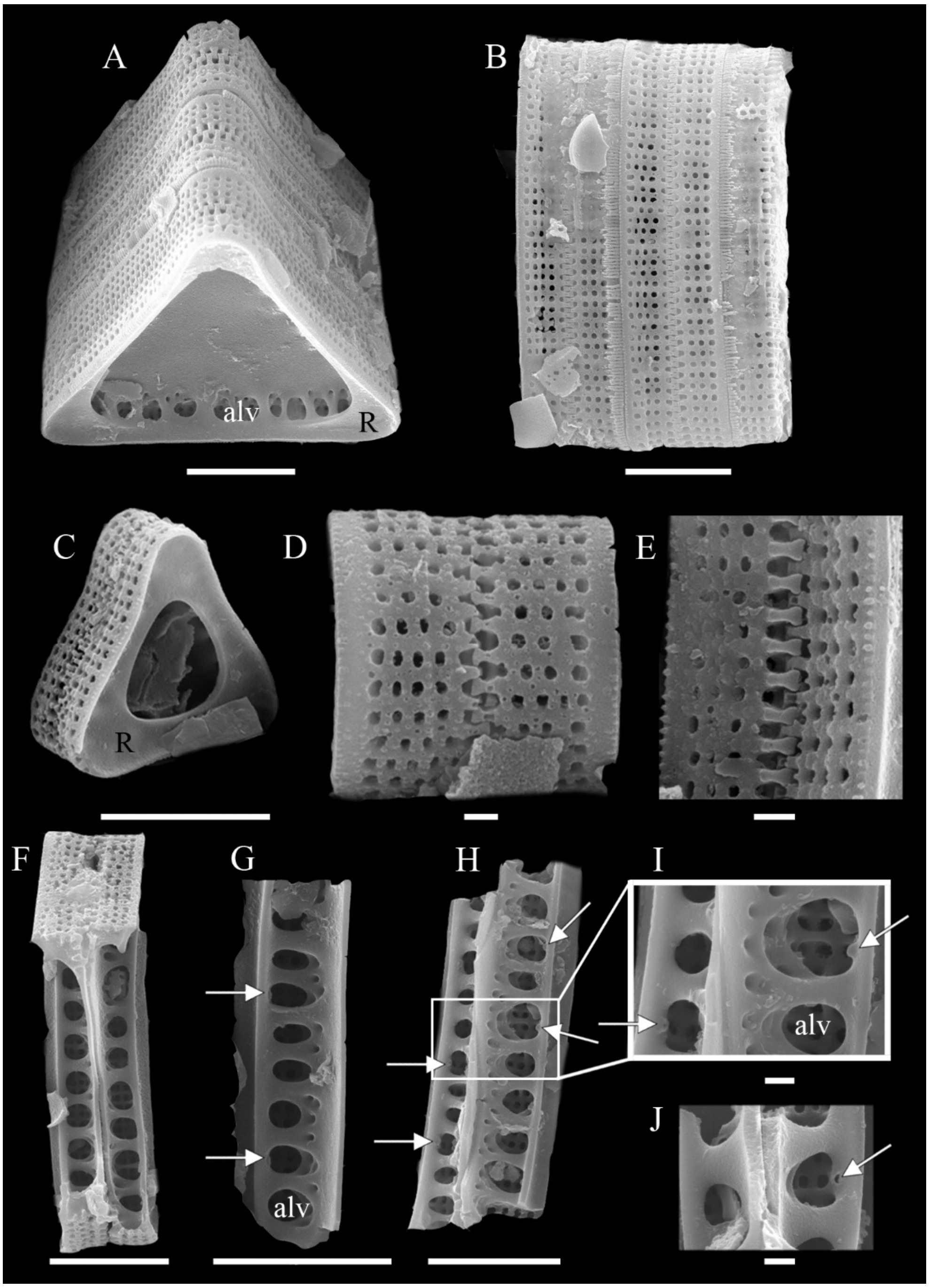

Figure 12. *Alveolophora antiqua* in the depth range of 48 to 44.5 m from core 517 of the Barguzin Valley: (**A**–**D**)—external views, showing variability of valves; (**E**)—linking spines; (**F**–**J**)—internal views, showing, alveolae and rimoportulae (arrows). SEM. Scale bar: 10 µm (**A**–**E**,**I**) and 1 µm (**F**–**H**,**J**).

A detailed study of *A. antiqua* morphological variability from different core horizons allowed us to establish an extended diagnosis for this species.

Alveolophora antiqua (Moisseeva) Moisseeva emend Usoltseva et Titova

Homotypic synonyms:

Melosira *antiqua* Moisseeva [10] (Figure 12, 7a–r), [11] (Table 1, 1, 2; 2, 1, 2)

Aulacosira antiqua (Moisseeva) Moisseeva [12] (p. 71).

Miosira antiqua (Moisseeva) Khursevich [13] (Table 150, 1, p. 112)

Diagnosis: The shape of the valves can be round, oval, ovoid or triangular. The valve diameter along the apical axis is 5–49 µm, and, along the transapical axis, it is 4–48 µm. The side length of triangular valves is 11–53 µm. The outer face of the valve in the center is smooth or covered with small granules. Areolae along the edge of valve face are located in 1–4 rows or are not present. The mantle height is 1.8–3.8 µm. Round areolae are located on the mantle in straight rows. The number of areola rows on the mantle is 11–15 in 10 µm, and areolae number 7–12 in 10 µm within a row. The areolae number in a row is 2–4. Linking spines are spathulate. Separating spines are elongated and petaloid. The ringleist varies from narrow to wide. The ringleist aperture can be round, ovoid, oval or triangular and varies in diameter from 2.6 to 16 µm along the apical axis and from 2 to 12 µm along the transapical axis. Well-developed alveolae interzones divided by costae are distinct in the valve interior. Costae number 3–6 in 10 µm. Rimoportulae are sessile, located at the base of alveolae, every 2–4 costae. Their external opening are associated with the first areola in a row.

Locality and age sediments: Russia: Early Miocene: Transbaikalia: Barguzinskaya Valley and Vitim Plateau; Late Miocene Baikal Lake.

4. Discussion

The description of the taxon *Alveolophora antiqua* was as follows. Shapes are triangular–oval and triangular with widely rounded corners, and the side length is 8.0–40.0 µm. Along the edge of the face part, pore valves are in short radial rows, 7–9 in 10 µm, alternated with short rib-like direct or slightly curved thickenings at each 2–4 pores rows. The center is structureless and torulose. Mantle is 4.0–8.0 µm high, with lengthwise direct pores in rows, 7–9 in 10 µm, with rib-like thickenings like on the valve face. The collum is low and structureless. The ringleist varies from narrow to rather wide (mainly in small specimens), with thin costae of different lengths along the external edge. Linking spines are very small [4] (pp. 542, Table I, 11–16).

In this work, we documented for the first time the valve morphology in this species using SEM. Specimens from different core horizons were observed, and based on our observations, we extended the diagnosis for this species with data on spine shape, alveolae structure, rimoportulae and the aperture of rimoportula.

It is revealed that this species has different valve types (round, oval, ovoid and triangular) and that their proportion varies with the core depth. Morphological parameters for each valve type are presented in Table 1.

Table 1. Morphological characters of relative Alveolophora species.

Taxon	*A. jouseana*	*A. baicalensis*	*A. antiqua*	*A. antiqua*	*A. antiqua*	*A. antiqua*	*A. antiqua*
Valve form	round	round	triangular–oval and triangular with widely rounded corners	triangular and triangular with widely rounded corners	ovoid	oval	round
Height of valves	2.0–7.0	1.0–5.0	4.0–8.0	2.3–3.0	2.3–2.7	3.2–3.8	2.5–3.0
Diameter of valve (µm)	8.0–31.0	6.0–25.0	–	–	9.0–27.0 a.a 6.5–24.0 t.a	5.0–22.0 a.a 4.0–16.0 t.a	13.0–33.0
Length of one side of the valve	–	–	8.0–40.0	8.0–53.0	–	–	–

Table 1. *Cont.*

Taxon	*A. jouseana*	*A. baicalensis*	*A. antiqua*	*A. antiqua*	*A. antiqua*	*A. antiqua*	*A. antiqua*
Number of areolar rows in 10 µm	8–12 straight rows, each 2–4 rows of areolae alternate with costae	10–14 straight rows, each 2–4 rows of areolae alternate with costae	7–9 straight rows, each 2–4 rows of areolae alternate with costae	11–15 straight rows, each 2–4 rows of areolae alternate with costae	12–14 straight rows, each 2–4 rows of areolae alternate with costae	12–14	12–14 straight rows, each 1–3 rows of areolae alternate with costae
Number of areolae in a row	3–5	2–5		2–4	2–4	3	2–4
Areolae on the valve face	over the entire surface, along the periphery in 1–3 areolae rows or completely absent. Sometimes has granules at the center or one ring of granules at the periphery.	areolae in the submarginal zone of the valve face in short radial rows alternating with rib-like thickenings	without areolae or only on the periphery. Sometimes has granules at the center.	without areolae or only on the periphery 1–4 rows. Valve surface smooth or with granules. Sometimes, one ring of granules at the periphery.	without areolae or only on the periphery 1–4 rows. Valve surface smooth or with granules	without areolae or only on the periphery 1–4 rows. Valve surface smooth	without areolae or only on the peripheral 1–4 rows. Valve surface smooth or with granules. Sometimes, one ring of granules at the periphery
Linking spines	short, spathulate–widened	spathulate	small	spathulate	spathulate	spathulate	spathulate
Separating spines	pointed	–	–	elongated petaloid	-	-	–
Ringleist	narrow	narrow	narrow–wide	narrow–wide	narrow–wide	narrow–wide	narrow–wide
Shape and diameter (µm) of ringleist aperture	big round or medium	big round or medium	triangular or oval	triangular with widely rounded corners 5.0–6.0 a.a 4.7 t.a	ovoid or oval, 2.3–16.0 a.a 2.0–12.0 t.a	oval, 3.5–8.0 a.a 2.7–5.0 t.a	round, 6.0–9.0
Rimoportulae	small, sessile, located at the base of the costae or pseudoalveolae	sessile, located at the base of pseudoalveolae	–	sessile, located at the base of alveolae, every 2–4 costae	sessile, located at the base of alveolae, every 2–4 costae	sessile, located at the base of alveolae, every 2–4 costae	–
Alveolar character	pseudoalveolae and micro-pseudoalveolae	pseudoalveolae	–	alveolae	alveolae	alveolae	alveolae
Number of costae in 10 µm	3–10	4–8 (12)	–	3–6	3–8	4–6	3–8
Location	Far East, Primorye, Lake Tony	Lake Baikal,	Transbaikalia, Vitim Plateau	Barguzin Valley, core 517	Barguzin Valley, core 517	Barguzin Valley, core 517	Barguzin Valley, core 517
Age	Miocene	Late Miocene	Early Miocene	Early Miocene	Early Miocene	Early Miocene	Early Miocene
References	[14]	[15]	[4]	present data	present data	present data	present data

Valves differing by shape had a different range of the morphological variability of morphometric parameters, such as valve height and diameter. For example, the oval valve height was a slightly greater (3.2–3.8 µm) than the heights in valves with triangular (2.3–3.0 µm), ovoid (2.5–3.0 µm) or round (2.3–2.7 µm) outlines. We measured diameter of round, oval and ovoid valves. Round valves had a maximum diameter of 33.0 µm. The diameters of oval and ovoid valves varied but were similar in size. As for triangular valves, we measured the length of the valve side, which varied from 8.0 to 53.0 µm. Other parameters for the valve types were all similar to one another (Table 1).

Some questions arise while comparing our data with the diagnosis [4]. First, valve height in the diagnosis is 4.0–8.0 µm; however, according to Table 1, Figures 5 and 11 in [4], with attention to the scale (10 µm), we can see that the valve height does not exceed 5.0 µm. Probably, the authors presented the size of the frustule comprising two valves. Therefore, we cannot consider these parameters as differing ones.

Second, the authors indicate, in the diagnosis, that there are 7–9 areolar rows with 10 µm, and according to our data, there are 11–15 with 10 µm. This is probably due to light microscopy studies done by the original authors. It is difficult to estimate their number in the figures 5 and 11 presented in the publication [4].

It is interesting that all figures in [4] are similar to the population which we studied in the depth range of 54 to 53 m from core 517. In the original description of valve shape, the authors noticed that valves were triangular–oval and triangular with widely rounded corners, and in their figures, there were also oval and ovoid valves as well (Table 1, Figures 14 and 15 in [4]).

To compare the species in question with taxa that are in our opinion morphologically similar, we used the species *A. jouseana* and *A. baicalensis* (Table 1). Although by valve size (height, diameter), these species are close to *Alveolophora antiqua*, they differ by the internal structure of the valve (having pseudoalveolae rather than alveolae). Differences from *Alveolophora antiqua* include that *A. jouseana* can have areolae on the whole surface of the face valve, separating spines are pointed and the rimoportulae are located at the base of costae.

According to our earlier studies of fossil deposits in the Baikal Region [1–3,16], the dominance of one species along the entire core can be observed rarely. In this work we have shown that the valve shape of the same species, *A. antiqua,* varies in the core with depth. Other authors noticed valve shape variation in the core of fossil deposits as well. For example, it is shown in [14] how valve shape varied in *Melosira* aff. *jouseana* Moisseeva. The authors distinguish perfect trilobate, sub-rectangular, triangular, bilobate and almost circular forms. These modifications are restricted to the shape of the frustules in valve view, and they do not affect the other morphological features of the valve. According to [17], the shape of the valves is a minor character that cannot be sufficient for specific separation. We agree with this statement of the authors.

However, we can state that non-circular valve shape is an indicator of ancient Miocene deposits because, in all modern species of Aulacoseiraceae Crawford, the frustule is circular in valve view. Besides *Alveolophora antiqua*, non-circular shapes occurred in the Miocene genera *Miosira* Krammer, Lange-Bertalot et Schiller, *Alveolophora* Moisseeva et Nevretdinova and *Aulacoseira* Thwaites. Among them, *Miosira rhoenana* Krammer, Lange-Bertalot et Schiller have trilobate, triangular and almost circular forms [18]. In addition, six taxa of elliptical (oval) *Aulacoseira* have been described, including: *A. ovata* Usoltseva et Tsoy and *A. elliptica* Tsoy et Usoltseva [19], *A. hachiyaensis* Tanaka [20], *A. iwakiensis* Tanaka et Nagumo [21], *Melosira distans* var. *ovata* and Iwahashi [22] *A. capitalina* Titova et Usoltseva [23].

A triangular valve shape is sometimes observed in other genera as well. Shrader [24] considered the triangular valves of *Stephanodiscus carconensis* Grunow to be abnormal forms and interpreted them as ecological modifications produced by restricted environmental conditions during the cold season. Similar valves forms have been recorded in *Stephanodiscus pontica* Jousé [25] and *Cyclotella* sp. [17].

It is curious that the triangular cells have higher volume than all other morphotypes; further, they immediately form the majority of the population as soon as they appear. One possible explanation is that their appearance was caused by the polyploidization of a previously existing morphotype. It is known that the increase in the amount of DNA per cell, either by polyploidization or through multiple smaller-scale events, leads to an increase in cell volume in diatoms [26] and that polyploidizations are abundant in ancient diatom evolution [27]. If such an event took place within the *A. antigua* population, it would have separated it into two isolated subpopulations not unlike modern *Ditylum brightwellii* (West) Grunow [28]. These populations would then compete with each other, and a polyploid triangular form could gain an adaptive advantage through the neofunctionalization of newly formed paralogs and the general rearrangement of transcriptional regulation that usually follows a change in karyotype. Although this hypothesis is highly speculative, it does fit all of the available evidence.

5. Conclusions

The morphology of *Alveolophora antiqua* (Moisseeva) Moisseeva from the freshwater Early Miocene paleolake in the Barguzin Valley was studied by scanning electron microscopy. We extended the species diagnosis and show a wide morphological variability with regard to valve shape (round, oval, ovoid and triangular). We have to notice that, in our samples, not only shape- but also size-varied. In lower horizons, valves were smaller than in upper ones. How can we explain the decrease or increase of planktonic diatoms sizes in a population? There may be several explanations for these observations. First, differences may be explained by the fact that cell size in diatoms can depend on their life cycle [29,30]. Diatoms can respond to the same condition by progressively reducing their cell size (asexual reproduction) or can restore their size by auxospore formation. Second, according to Winder et al. [31], the size of planktonic diatoms decreases with climate warming because of the reduced nutrient redistribution and the increasing sinking velocities. Their results show that, within the diverse group of diatoms, small-sized species with a high surface-area-to-volume ratio were able to adapt to a decrease in mixing intensity, supporting the hypotheses that abiotic drivers affect the size structure of planktonic communities and that a warmer climate favors small-sized diatom cells [31]. Other studies revealed that larger *Rhizosolenia* Brightwell specimens occur in sites with lower temperatures [32]. Size variations at the level of species have also been recorded for other aquatic and terrestrial organisms [33]. For example, in anurans, it is known that low temperatures may influence growth and development rates in larval and juvenile stages, which have follow-on effects on maturity and growth, and consequently high-latitude and -altitude individuals should be generally larger than low-latitude and tropical specimens [34,35]. Lower temperatures trigger a similar effect in marine invertebrates [36,37], fish [38,39], arthropods [40,41] and other amphibians [42,43].

Currently we cannot tell exactly which climatic or tectonic events could affect the variation in valve shape in the *A. antiqua* population studied herein. According to lithological and palynological data [6], no particular changes occurred in the interval of transition from oval valves to triangular ones. However, data on diatom shape and sizes can suggest changes in habitat conditions towards cooling during the Early Miocene.

Author Contributions: Conceptualization M.U.; collected samples, M.U. and S.R.; microscopy and data analysis, M.U., A.H. and L.T.; graphic analysis, A.M.; interpretation of the results, M.U., L.T. and A.M.; project administration, M.U.; writing—original draft preparation, M.U., A.H. and L.T.; writing—review and editing, M.U., A.H., L.T., A.M. and S.R. All authors have read and agreed to the published version of the manuscript.

Funding: The investigation was done with the financial support of the State Assignments of the Limnological Institute of the Siberian Branch of the Russian Academy of Sciences #0279-2021-0008 (121032300186-9).

Institutional Review Board Statement: Not applicable.

Informed Consent Statement: Not applicable.

Data Availability Statement: Not applicable.

Acknowledgments: The authors are grateful to S. Reshetova (A.P. Vinogradov Institute of Geochemistry, Siberian Branch of the RAS, Russia) for the discussion of the palynological data and Patrick Kociolek and Yulia Kaplyukova for English translation. The study was performed using microscopes of the Instrumental Centre "Electron Microscopy" (http://www.lin.irk.ru/copp/) of the Shared Research Facilities for Research "Ultramicroanalysis".

Conflicts of Interest: The authors declare no conflict of interest.

References

1. Hassan, A.; Usoltseva, M.V.; Rasskazov, S.V.; Chuvashova, I.S.; Titova, L.A. First study of fossil diatom flora from Middle Miocene-Lower Pliocene lacustrine sediments in Barguzin Valley, Baikal Rift Zone. *Quart. Int.* **2019**, *524*, 24–30. [CrossRef]
2. Usoltseva, M.V.; Titova, L.A.; Hassan, A.; Chuvashova, I.S.; Rasskazov, S.V. Centric diatoms from paleolakes of the Baikal Rift Zone, Russia. *Issues Mod. Algol.* **2019**, *2*, 279–284. (In Russian) [CrossRef]
3. Usoltseva, M.V.; Hassan, A.; Rodionova, E.V.; Titova, L.A.; Chuvashova, I.S.; Rasskazov, S.V. The first finding of diatoms from the Early Miocene lacustrine deposits of the Barguzin Valley (Baikal Rift Zone). *Limnol. Freshw. Biol.* **2020**, *4*, 752–754. [CrossRef]
4. Moisseeva, A.I.; Nevretdinova, T.L. The new family and genus of fresh water diatom algae (Bacillariophyta). *Bot. Zhurnal* **1990**, *75*, 539–544. (In Russian)
5. Glezer, S.I.; Makarova, I.V.; Moisseeva, A.I.; Nikolaev, V.A. *The Diatoms of the USSR Fossil and Recent*; Nauka St.-Petersburg Branch: St. Petersburg, Russia, 1992; Volume 2, Fasc. 2, p. 126. (In Russian)
6. Kuz'min, M.I.; Khursevich, G.K.; Prokopenko, A.A.; Sedenya, S.A.; Karabanov, E.B. *Late Cenozoic Centric Diatoms of Lake Baikal*; Academic Publishing House Geo: Novosibirsk, Russia, 2009; p. 370. (In Russian)
7. Hassan, A.I.; Rasskazov, S.V.; Chuvashova, I.S.; Reshetova, S.A.; Rubcova, M.N.; Yasnygina, T.A.; Budaev, R.C.; Al'Hamud, A.; Titova, L.A.; Rodionova, E.V.; et al. Cenozoic sediments from the Selenga-Vitim Downwarp and Baikal Rift Zone spatially combined in the Uro section. *Litosfera* 2022, 6, *in press*. (In Russian)
8. Grachev, M.A.; Vorobyova, S.S.; Likhoshway, Y.V.; Goldberg, E.L.; Ziborova, G.A.; Levina, O.V.; Khlystov, O.M. A high resolution diatom record of the palaeoclimates of East Siberia for the last 2.5 my from Lake Baikal. *Quat. Sci. Rev.* **1998**, *17*, 1101–1106. [CrossRef]
9. Hunter, J.D. Matplotlib: A 2D graphics environment. *Comput. Sci. Eng.* **2007**, *9*, 90–95. [CrossRef]
10. Jouse, A.P. The Bacillariophyta, Class Centricae. In *Fundamentals of Palaeontology, A Reference Book for the Palaeontologists and Geologists of the USSR*; Orlov, U.A., Ed.; Academy of Sciences of the USSR: Moscow, Russia, 1963; pp. 55–121. (In Russian)
11. Jouse, A.P. Diatomeen in Seesedimenten. *Arch. Fur Hydrobiol. Beihandlungen Ergeb. Limnol.* **1966**, *4*, 1–32. (In Russian)
12. Moiseeva, A.I. Revision of the systematic position of freshwater species of the genus *Melosira* Ag. s. l. (Bacillariophyta). In *Sbornik Nauchnykh Trudov. Aktual'nye Voprosy Sovremennoi Paleoalgologii*; Sokolov, B.S., Ed.; Naukova Dumka: Kiev, Ukraine, 1986; pp. 70–73. (In Russian)
13. Kozyrenko, T.; Strelnikova, N.; Khursevich, G.; Tsoy, I.; Yakovschikova, T.; Mukhina, V.; Olshtynskaja, A.; Semina, G. *The Diatoms of Russia and Adjacent Countries Fossil and Recent II*; Strelnikova, N., Tsoy, I., Eds.; St. Petersburg University Press: St. Petersburg, Russia, 2008; p. 171. (In Russian)
14. Usoltseva, M.V. Morphological variability of *Alveolophora jouseana* (Bacillariophyta) from type material. *Phytotaxa* **2022**, *533*, 194–204. [CrossRef]
15. Khursevich, G.K.; Fedenya, S.A. Morphology of new fossil species of *Concentrodiscus* and *Alveolophora* (Bacillariophyta) from bottom sediment of Lake Baikal. *Int. J. Algae* **2006**, *8*, 78–90. [CrossRef]
16. Titova, L.A.; Hassan, A.; Mikhailov, I.S.; Rodionova, E.V.; Rasskazov, S.V.; Usoltseva, M.V. Diversity and Ecology of Diatoms in Pliocene Deposits of the Tunka Valley (Baikal Rift Zone). *Diversity* **2021**, *13*, 479. [CrossRef]
17. Servant-Vildary, S.; Paicheler, J.C.; Semelin, B. *Miocene lacustrine Diatom from Turkey, Proceedings of the 9th International Diatom Symposium, Bristol, UK, 24–30 August 1986*; Round, F.E., Ed.; Biopress, Ltd.: Bristol, UK; Koeltz, Koenigstein: Bristol, UK, 1986; pp. 165–180.
18. Krammer, K. *Die Cymbelloiden Diatomeen, Teil 2. Encyonema Part. Encyonopsis und Cymbellopsis, Bibliotheca Diamotologica Bd. 37*; Cramer, J., Ed.; Schweizerbart Science Publishers: Berlin, Germany; Stuttgart, Germany, 1997; p. 469.
19. Usoltseva, M.V.; Tsoy, I.B. Elliptical species of the freshwater genus *Aulacoseira* in Miocene sediments from Yamato Rise (Sea of Japan). *Diatom Res.* **2010**, *25*, 397–415. [CrossRef]
20. Tanaka, H.; Nagumo., T.; Akiba, F. *Aulacoseira hachiyaensis* sp. nov., A new Early Miocene freshwater fossil diatom from Hachiya Formation, Japan. In Proceedings of the 19th International Diatom Symposium, Irkutsk, Russia, 28 August–3 September 2006; Biopress: Bristol, UK, 2008; pp. 115–123.
21. Tanaka, H.; Nagumo, T. *Aulacoseira iwakiensis* Sp. Nov., A New Elliptical *Aulacoseira* Species, From an Early Miocene Sediment, Japan. *Diatom* **2011**, *27*, 1–8.
22. Iwahashi, Y. Freshwater Centricae in Japan (Iv). *J. Jpn. Bot.* **1935**, *11*, 768–771. (In Japanese)

23. Titova, L.A.; Hassan, A.; Usoltseva, M. *Aulacoseira capitalina* sp. nov. (Bacillariophyta) from the Middle Miocene sediments of the Barguzin Valley, Baikal Rift Zone (Russia). *Acta Biol. Sibirica* **2022**, *8*, 571–582. (In Russian) [CrossRef]
24. Schrader, H.J. Quaternary through Neogene history of the Black Sea, deduced from the paleoecology of diatoms, silicoflagellates, ebridians, and chrysomonads. In *Initial Reports of the Deep-Sea Drilling Project*; Ross, D.A., Neprochnov, Y.P., Eds.; U.S. Government Printing Office: Washington, DC, USA, 1978; Volume 42, pp. 789–901.
25. Jouse, A.P.; Mukhina, V.V. Diatoms units and the paleogeography of the Black Sea in the late Cenozoic. DSDP. In *Initial Reports of the Deep-Sea Drilling Project*; Ross, D.A., Neprochnov, Y.P., Eds.; U.S. Government Printing Office: Washington, DC, USA, 1978; pp. 903–950.
26. Connolly, J.A.; Oliver, M.J.; Beaulieu, J.M.; Knight, C.A.; Tomanek, L.; Moline, M.A. Correlated evolution of genome size and cell volume in diatoms (Bacillariophyceae). *J. Phycol.* **2008**, *44*, 124–131. [CrossRef] [PubMed]
27. Parks, M.B.; Nakov, T.; Ruck, E.C.; Wickett, N.J.; Alverson, A.J. Phylogenomics reveals an extensive history of genome duplication in diatoms (Bacillariophyta). *Am. J. Bot.* **2018**, *105*, 330–347. [CrossRef] [PubMed]
28. Koester, J.A.; Swalwell, J.E.; Von Dassow, P.; Armbrust, E. Genome size differentiates co-occurring populations of the planktonic diatom *Ditylum brightwellii* (Bacillariophyta). *BMC Evol. Biol.* **2010**, *10*, 1. [CrossRef]
29. Round, F.E.; Crawford, R.M.; Mann, D.G. *The Diatoms: Biology and Morphology of the Genera*; Cambridge University Press: Cambridge, UK, 1990; p. 747.
30. Mann, D.G.; Chepurnov, V.A.; Droop, S.J.M. Sexuality, incompatibility, size variation, and preferential polyandry in natural populations and clones of *Sellaphora pupula* (Bacillariophyceae). *J. Phycol.* **1999**, *35*, 152–170. [CrossRef]
31. Winder, M.; Reuter, J.E.; Schlado, S.G. Lake warming favours small-sized planktonic diatom species. *Proc. R. Soc.* **2008**, *276*, 427–435. [CrossRef]
32. Wimpenny, R. The Size of Diatoms. I. The Diameter Variation of *Rhizosolenia Styliformis Brightw.* and *R. Alata Brightw.* in Particular and of Pelagic Marine Diatoms in General. *J. Mar. Biol. Assoc. U. K.* **1936**, *21*, 29–60. [CrossRef]
33. Pinto, R.; Mortágua, A.; Almeida, S.F.P.; Serra, S.; Feio, M.J. Diatom size plasticity at regional and global scales. *Limnetica* **2020**, *39*, 387–403. [CrossRef]
34. Berven, K.A. The genetic basis of altitudinal variation in the wood frog Rana sylvatica. I. An experimental analysis of life history traits. *Evolution* **1982**, *36*, 962–983. [CrossRef]
35. Zhong, M.; Yu, X.; Liao, W. A Review for Life-history Traits Variation in Frogs Especially for Anurans in China. *Asian Herpatol. Res.* **2018**, *9*, 165–174. [CrossRef]
36. Irie, T.; Fischer, K. Ectotherms with a calcareous exoskeleton follow the tempera_ture-size rule-evidence from field survey. *Mar. Ecol. Prog. Ser.* **2009**, *385*, 33–37. [CrossRef]
37. Daufresne, M.; Lengfellner, K.; Sommer, U. Global warming benefits the small in aquatic ecosystems. *Proc. Natl. Acad. Sci. USA* **2009**, *106*, 12788–12793. [CrossRef]
38. Desai, A.S.; Singh, R.K. The effects of water temperature and ration size on growth and body composition of fry of common carp, *Cyprinus carpio*. *J. Therm. Biol.* **2009**, *34*, 276–280. [CrossRef]
39. Sahin, T. Effect of water temperature on growth of hatchery reared Black Sea turbot, Scophthalmus maximus (Linnaeus, 1758). *Turk. J. Zool.* **2001**, *25*, 183–186.
40. Stillwell, R.C.; Fox, C.W. Geographic variation in body size, sexual size dimorphism and fitness components of a seed beetle: Local adaptation versus phenotypic plasticity. *Oikos* **2009**, *118*, 703–712. [CrossRef]
41. Brehm, G.; Zeuss, D.; Colwell, R.K. Moth body size increases with elevation along a complete tropical elevational gradient for two hyperdiverse clades. *Ecography* **2018**, *42*, 632–642. [CrossRef]
42. Bizer, J.R. Growth rates and size at metamorphosis of high elevation populations of *Ambystoma tigrinum*. *Oecologia* **1978**, *34*, 175–184. [CrossRef] [PubMed]
43. Schäuble, C.S. Variation in body size and sexual dimorphism across geographical and environmental space in the frogs *Limnodynastes tasmaniensis* and *L. peronei*. *Biol. J. Linn. Soc.* **2004**, *82*, 39–56. [CrossRef]